On the Performance of Rate 1/2 Convolutional Codes with QPSK on Rician Fading Channels

YUH-LONG CHEN, MEMBER, IEEE, AND CHE-HO WEI, SENIOR MEMBER, IEEE

***Abstract*—This paper is concerned with the bit error probability performance of rate 1/2 convolutional codes in conjunction with quaternary phase shift keying (QPSK) modulation and maximum likelihood Viterbi decoding on fully interleaved Rician fading channels. Applying the generating function union bounding approach, an asymptotically tight analytic upper bound on the bit error probability performance is developed under the assumption of using the Viterbi decoder with perfect fading amplitude measurement. Bit error probability performance of constraint length K = three to seven codes with QPSK is numerically evaluated using the developed bound. Tightness of the bound is examined by means of computer simulation. The influence of perfect amplitude measurement on the performance of Viterbi decoder is also observed. Finally, performance comparison with rate 1/2 codes with binary phase shift keying (BPSK) is also provided.**

I. Introduction

DIGITAL COMMUNICATIONS over mobile channels often suffer from multipath effects, which result in signal fading. Multipath fading plagues the propagation medium by imposing random amplitude and phase variations onto the transmitted waveform. For satellite-aided mobile communications, the channels can be modeled, in most cases, as nonfrequency selective Rician channels for which the fading amplitude obeys a Rician distribution. It is known that this fading degrades the performance of communication systems. The fade margin for uncoded binary phase shifted keying (BPSK) and quaternary phase shift keying (QPSK) systems on channel impaired by Rician fading has been examined in [1]. To combat Rician fading, convolutional codes with Viterbi decoding and interleaving could be used. The performance of short constraint length convolutional codes in conjunction with BPSK modulation and various types of maximum likelihood (ML) Viterbi decoding on Rician channels has been studied in detail [2]–[5]. The studies indicate that, of the various types of Viterbi decoder, the one utilizing full channel state information, channel fading amplitude, and phase, contributes the best performance.

With BPSK modulation, the code redundancy introduced by convolutional coding represents a bandwidth sacrifice in that the ratio of required bandwidth to information rate is increased. To avoid this sacrifice in bandwidth efficiency and also provide effective error-control protection, convolutional codes with multilevel modulation could be used instead. Error performance of convolutional codes with M-ary PSK modulation and Viterbi decoding on Rician/Rayleigh fading channels has been studied recently [6], [7]. An analytic upper bound on the bit error probability performance was developed and evaluated along with the studies. Simulation results show that the developed bound is somewhat loose for rate 1/2 convolutional codes with QPSK modulation on the mentioned channels.

In this paper, bit error probability performance of rate 1/2 short constraint-length convolutional codes with QPSK modulation and ML Viterbi decoding on Rician fading channels will be examined further because: 1) these codes are the most popular convolutional codes, and monolithic IC are commercially available for Viterbi decoders of constraint length K = six and seven codes; 2) rate 1/2 FEC codes with QPSK have been proposed for the second generation Inmarsat maritime satellite communication systems [8]. Our primary interest is in developing a tight performance bound on the bit error probability of convolutional codes with QPSK and in the performance comparison between convolutional codes with BPSK and QPSK. In Section II, the system under consideration, including the channel, is described. In Section III, applying the generation function union bounding approach, an analytic upper bound on the bit error probability performance is developed. For the convenience of derivation, we assume that the Viterbi decoder with perfect fading amplitude measurement is used. In Section IV, bit error probability performance of constraint length K = three to seven codes are numerically evaluated using the derived bound. Moreover, simulation results are provided for examining the tightness of the analytic bound. The influence of perfect fading amplitude measurement on the performance of Viterbi decoder is also observed. Finally, performance comparison with rate 1/2 convolutional codes with BPSK is made in Section V.

II. System Description

The block diagram of the system under consideration is shown in Fig. 1. The data bit u_i is encoded into a dibit $w_i = (w_{i1}, w_{i2})$ by a rate 1/2 convolutional encoder. The dibit is assigned to (using Gray mapping) a phase $\theta_i \in \{0, \pi/2, \pi, 3\pi/2\}$ which is corresponding to a signal point $x_i = \exp(j\theta_i)$ on the normalized signal space. After fully interleaving, the sequence $x = \{x_i\}$ is transformed into a time-domain waveform $s(t)$ by the QPSK modulator. The

Manuscript received August 11, 1986; revised September 25, 1989. This work was supported by the National Science Council of the Republic of China under Contract NSC78-0404-E009-32.

The authors are with the Institute of Electronics, National Chiao Tung University, Hsin-Chu, Taiwan, Republic of China.

IEEE Log Number 9034219.

0018-9545/90/0500-0161$01.00

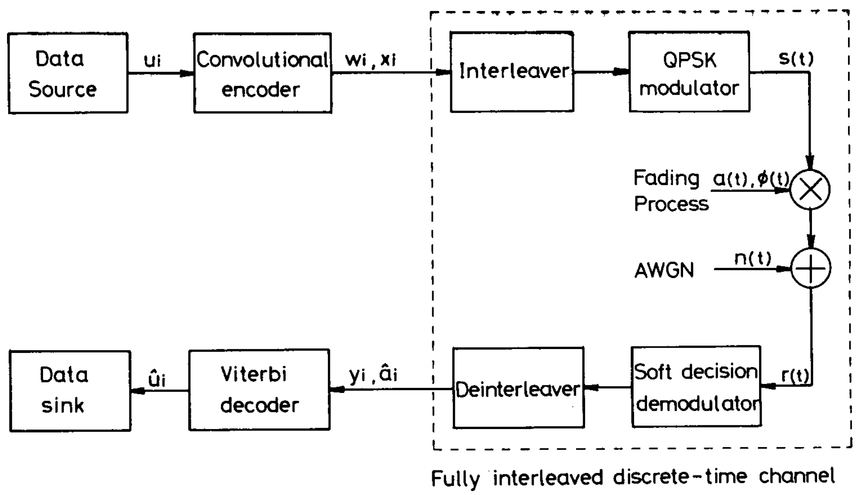

Fig. 1. Block diagram of the system under consideration.

transmitted signal $s(t)$ can be expressed as

$$s(t) = \mathrm{Re}\,\{g(t)e^{j\omega_0 t}\}. \tag{1}$$

where ω_0 is the carrier frequency, and $g(t)$ is the complex envelope given by

$$g(t) = \sqrt{2E_s}\sum_i \tilde{x}_i g_0(t - iT_s). \tag{2}$$

Here $\tilde{x}_i$ represents the interleaved version of x_i, $g_0(t)$ is the complex envelope of the transmitted signal with duration T_s and unit energy, and E_s represents signal energy per channel symbol. Since each data bit corresponds to a channel symbol, E_s equals the signal energy per bit E_b.

Passing through the Rician channel, transmitted signal $s(t)$ is corrupted by multipath fading resultant from the receiving of a stable specular (direct) component and a random diffuse (multipath) component. This fading, imposes random amplitude $a(t)$ and phase $\phi(t)$ onto $s(t)$. Besides fading, the transmitted signal is also corrupted by additive white Gaussian noise (AWGN) $n(t)$ with double-sided power spectral density $N_0/2$. The received signal $r(t)$ hence can be described by

$$r(t) = \mathrm{Re}\,\{a(t)e^{j\phi(t)}g(t)e^{j\omega_0 t}\} + n(t) \tag{3}$$

$$= \mathrm{Re}\,\{(\gamma e^{j\psi} + c(t))g(t)e^{j\omega_0 t}\} + n(t). \tag{4}$$

$\gamma e^{j\psi}$ is the specular component and $c(t)$ is the diffuse component. The specular component is a complex quantity whose amplitude γ is a fixed deterministic quantity while the phase ψ is uniformly distributed over $[-\pi, \pi]$. The diffuse component can be modeled as individual quadrature components that are Gaussian with zero mean and common variance σ^2. The amplitude process $a(t)$ then possesses the Rician distribution

$$f(a) = \frac{a}{\sigma^2}\exp\left\{-\frac{a^2+\gamma^2}{2\sigma^2}\right\} I_0\left(\frac{a\gamma}{\sigma^2}\right) \tag{5}$$

where $I_0(\cdot)$ is the modified Bessel function of the first kind of order zero. We will assume that the fading varies slowly compared to the signaling rate so that the channel amplitude $a(t)$ is constant during one signal interval of duration T_s. Moreover, for the convenience of analysis in the next section, we impose the following normalization

$$E[a^2] = \gamma^2 + 2\sigma^2 = 1 \tag{6}$$

so that the received energy per channel symbol is E_s and represents the sum of the corresponding specular and diffuse energy. The Rice factor defined by $\zeta = \gamma^2/2\sigma^2$ denotes the ratio of specular to diffuse energy. It is an important channel parameter in describing the channel. The distribution function for $a(t)$ can also be completely characterized in terms of ζ as

$$f(a) = 2a(1+\zeta)\exp\{-(1+\zeta)a^2 - a\}I_0(2a\sqrt{\zeta(1+\zeta)}). \tag{7}$$

The distribution $f(a)$ is sufficiently general, since as the parameter ζ approaches zero we have the Rayleigh channel, while if ζ approaches infinite the Rician channel reduces to the nonfading Gaussian channel (AWGN channel) with $a = 1$.

The received signal is coherently demodulated by a soft decision, optimum demodulator under the assumption of perfect timing recovery and exact tracking of the carrier phase. The output of the deinterleaver, relevant to the transmitted x_i, is the normalized decision variable y_i given by

$$y_i = \sqrt{\frac{E_b}{N_0}}a_i x_i + N_i. \tag{8}$$

Here $\{N_i\}$ is an independent identically distributed (iid) sequence of complex Gaussian variates with zero mean and unit variance. $\{a_i\}$ is also an iid sequence of Rician variates with distribution specified by (5). The decision variable y_i is supplied to the Viterbi decoder. In addition to $\boldsymbol{y} = \{y_i\}$ the Viterbi decoder with perfect amplitude measurement is also supplied with $\boldsymbol{a} = \{a_i\}$, the channel amplitude estimates, from a channel estimator. The Viterbi decoder performs ML decoding and recovers the transmitted data.

III. Performance Bound

In determining the bit error probability performance bound of convolutional codes with Viterbi decoding, it is useful to recall the generating function union bounding approach [9]. Therefore, the pairwise error probability between the transmitted sequence and the estimated sequence must be first developed. Moreover, for the convenience of deriving the analytic expression of the pairwise error probability, we assume that the Viterbi decoder with perfect amplitude measurement is used. For such an ML Viterbi decoder, the decision rule between possible transmitted sequences $\boldsymbol{x} = \{x_i\}$ and $\boldsymbol{x}' = \{x_i'\}$ given the received sequences $\boldsymbol{y} = \{y_i\}$ and $\boldsymbol{a} = \{a_i\}$ is (derived in Appendix I)

$$\hat{\boldsymbol{x}} = \boldsymbol{x}', \quad \text{if} \sum_i a_i y_i (x_i - x_i')^* + a_i y_i^* (x_i - x_i') < 0 \quad (9)$$

where $\hat{\boldsymbol{x}}$ denotes the estimated sequence of the decoder and the asterisk denotes the operation of complex conjugate.

We may assume, without lose of generality, that the sequence $\boldsymbol{x} = \{x_i\}$, with $x_i = 1$, relevant to the all-zero message is the transmitted sequence. For the estimated sequence $\hat{\boldsymbol{x}}$ (which differs from the transmitted sequence $\boldsymbol{x}$ in exact k symbol positions and of these k symbols there are k_1 symbols with value $\pm j$ and k_2 symbols with value -1), the unconditional pairwise error probability $P_{k_1 k_2}$ for such estimated sequence is derived in Appendix II. It is bounded by

$$P_{k_1 k_2} \le C_0 Z_1^{k_1} Z_2^{k_2}. \quad (10)$$

where C_0 depends on the code and the channel used. Z_1 and Z_2 are given by

$$Z_1 = \frac{1}{1 + \frac{E_b}{2N_0}\frac{1}{1+\zeta}} \exp\left(\frac{-\frac{E_b}{2N_0}\frac{\zeta}{1+\zeta}}{1 + \frac{E_b}{2N_0}\frac{1}{1+\zeta}} \right) \quad (11a)$$

$$Z_2 = \frac{1}{1 + \frac{E_b}{2N_0}\frac{1}{1+\zeta}} \exp\left(\frac{-\frac{E_b}{N_0}\frac{\zeta}{1+\zeta}}{1 + \frac{E_b}{N_0}\frac{1}{1+\zeta}} \right). \quad (11b)$$

For rate 1/2, k = three to eight optimum convolutional codes [10], factor C_0 obtained in Appendix II is given below

$$C_0 = E\left[Q\left(\sqrt{\frac{2E_b}{N_0} \sum_{i=1}^{2} a_i^2} \right) \right] \quad (12)$$

where $Q(z) = 1/\sqrt{2\pi} \int_z^\infty e^{-w^2/2}\, dw$.

At this point, the union bound is then used to upperbound the bit error probability P_b. We have

$$P_b \le \sum_i \sum_{k_1} \sum_{k_2} i a(k_1, k_2, i) P_{k_1 k_2} \quad (13)$$

where $1(k_1, k_2, i)$ is the number of sequences with both error pattern (k_1, k_2) and i bit error. This information can be determined from the augmented generating function associated with the particular code employed. To deduce the augmented generation functions such that it contains $a(k_1, k_2, i)$, the modified state diagram is used and must be properly labeled. For expository purposes, rate 1/2, constraint length $K = 3$, convolutional code with Gray mapping into QPSK is given as an example. Figs. 2(a) and 2(b) show the encoder and the state diagram of the code. Fig. 2(c) gives the QPSK signal space. Modified state diagram of the code is illustrated in Fig. 2(d). The branches of this diagram are labeled as either $D_0 = 1$, D_1, or D_2, if the relevant transmitted symbol associated with the particular branch is 1, $\pm j$, or -1, respectively. If the branch transition was caused by an input data "1," an additional factor I is introduced to the branch. From this labeled state diagram, a set of state equations is obtained and the augmented generating function is derived. In general, for rate 1/2 convolutional codes with QPSK, the augmented generating function can always be expressed as

$$T(D_1, D_2, I) = \sum_i \sum_{k_1} \sum_{k_2} a(k_1, k_2, i) I^i D_1^{k_1} D_2^{k_2}. \quad (14)$$

Partial derivative of $T(D_1, D_2, I)$ with respect to I at $I = 1$ becomes

$$\left.\frac{\partial T(D_1, D_2, I)}{\partial I}\right|_I = 1 = \sum_i \sum_{k_1} \sum_{k_2} i a(k_1, k_2, i) D_1^{k_1} D_2^{k_2}. \quad (15)$$

Substituting the result of (10) into (13) and comparing with (15), we obtain the desired bit error probability upper bound

$$P_b \le C_0 \left.\frac{\partial T(D_1, D_2, I)}{\partial I}\right|_{I=1, D_1=Z_1, D_2=Z_2}. \quad (16)$$

Z_1 and Z_2 are given by (11a) and (11b), respectively. For constraint length K = three to eight codes, C_0 is given by (12).

IV. Numerical and Simulation Results

In evaluating the bit error probability performance we utilize the analytic bound (16). A computer program has been developed to compute numerically $\partial T(D_1, D_2, I)/\partial I$ at $I = 1$ and hence to determine the analytic bound for the selected convolutional codes.

Due to practical interest, only the rate 1/2, constraint length K = three to seven, optimum codes with Gray mapping into QPSK are evaluated. Figs. 3 and 4 show the computed upper bounds for channel with Rice factor $\zeta = 0$ and 10 (severe and medium fading) respectively. It is found that each increment in K provides an improvement in performance and that the performance improvement versus K increases with decreasing bit error probability. Typical behavior with various ζ (from severe fading to nonfading case) is given in Figs. 5 and 6 for K = four and seven codes, respectively. Comparing with the

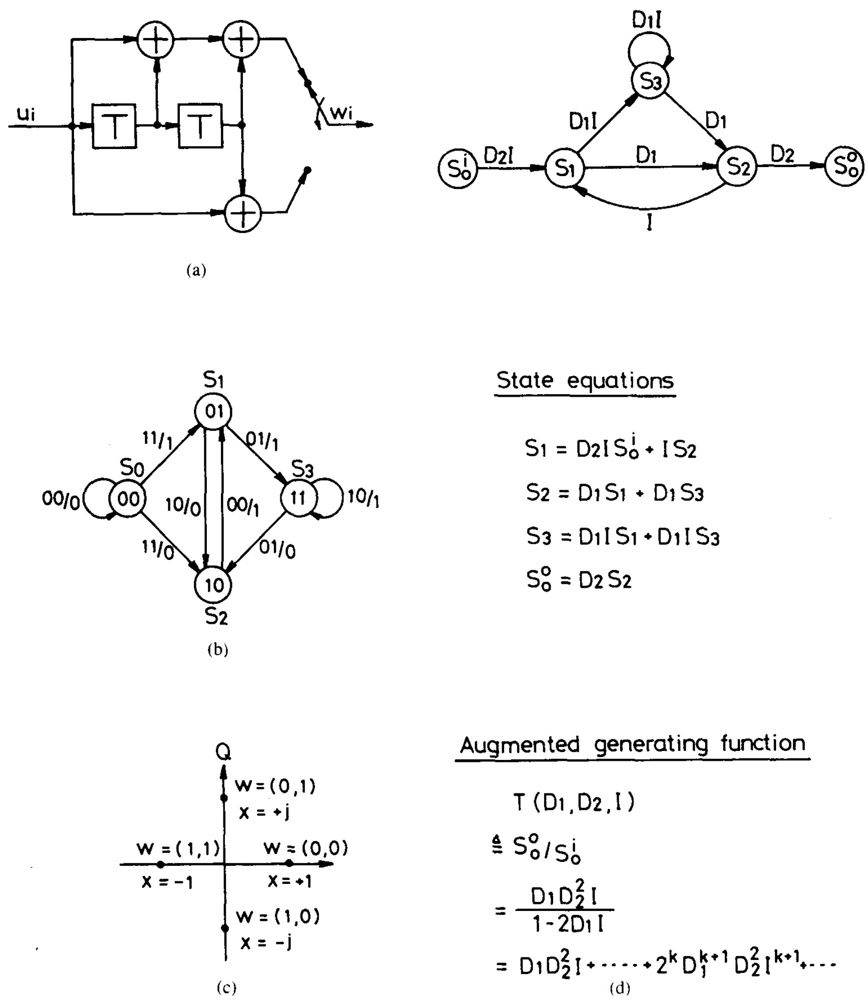

Fig. 2. (a) Rate 1/2, K = three, convolutional encoder. (b) State diagram of the code. (c) Signal space of QPSK with Gray mapping. (d) Modified state diagram and augmented generating function of the code with Gray mapping into QPSK.

nonfading performance curves, we found that the performance degradation is large, medium, and small for ζ in the range of $\zeta < 5$, $5 < \zeta < 20$, and $20 < \zeta$, respectively.

Tightness of the analytic bound and the influence of channel amplitude measurement on the decoder performance are further investigated using Monte Carlo computer simulation. In the simulation, the Viterbi decoder is supplied with infinitely finely quantized receiver output and the decoding depth of the decoder is six times the code memory. Both the Viterbi decoder with perfect amplitude measurement and that without amplitude measurement are used. The decoding rule for decoder without amplitude measurement is similar to (9) except that the amplitude weighting factor a_i is set to 1. Figs. 7 and 8 show the simulation results and the corresponding upper bounds for K = four and seven codes with QPSK on channels with $\zeta = 0$ and 10, respectively. The following points are observed from the performance curves.

1) The computed upper bounds are in good agreement with the simulation results for P_b approaching 10^{-4}. The generating function bound is asymptotically tight and the performance can be ascertained accurately for low P_b even in the absence of simulation.

2) Viterbi decoder with perfect amplitude measurement has better performance than that without amplitude measurement. About 1–2 dB relative performance improvement can be gained when fading is severe. For medium fading the relative improvement is small, hence the Viterbi decoder without amplitude measurement is good enough in most cases and the generating function bound can be applied as well to evaluate the performance of convolutional codes with such decoder.

V. Performance Comparison Between Convolutional Codes with BPSK and QPSK

Bit error performance of rate 1/2 convolutional codes with BPSK modulation and ML Viterbi decoding which makes perfect amplitude measurement has been studied [3]. For such decoder, the generating function bound on the P_b given in

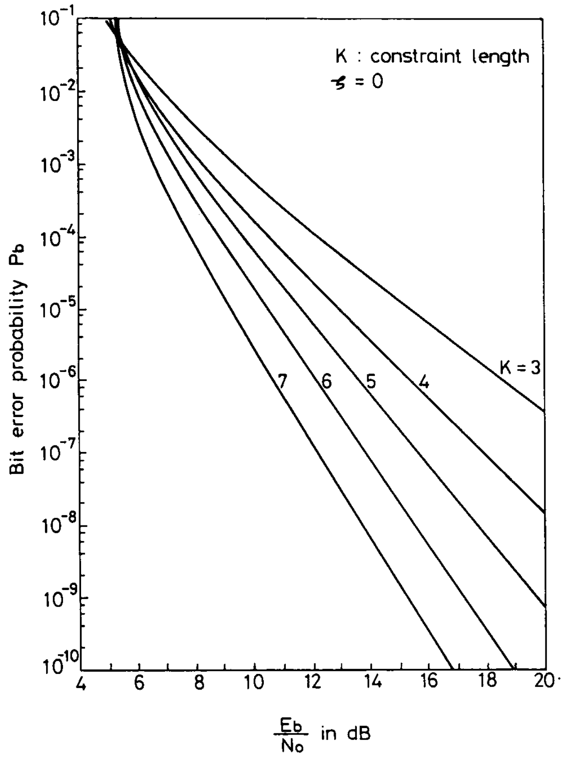

Fig. 3. Computed upper bounds for selected rate 1/2 codes with QPSK on fully interleaved Rician channel with $\zeta = 10$.

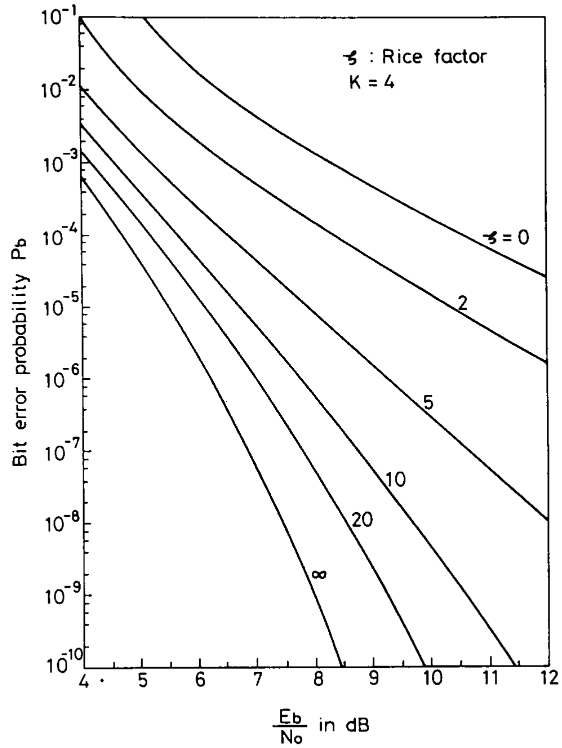

Fig. 5. Computed upper bounds for rate 1/2, K = four, optimum code with QPSK on fully interleaved Rician channel with $\zeta = 0, 2, 5, 10, 20, \infty$.

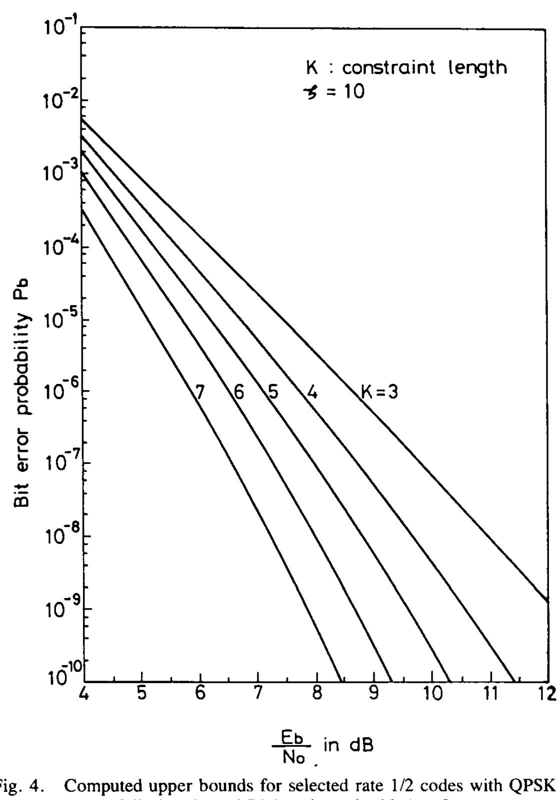

Fig. 4. Computed upper bounds for selected rate 1/2 codes with QPSK on fully interleaved Rician channel with $\zeta = 0$.

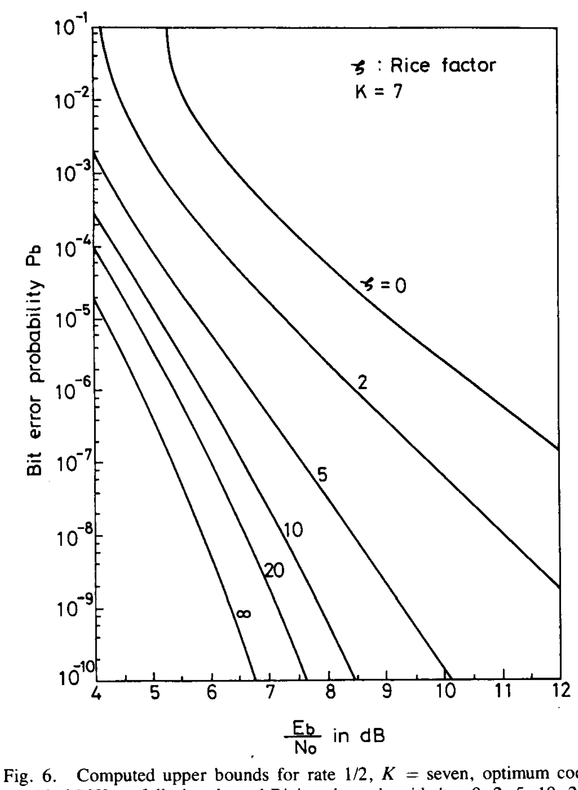

Fig. 6. Computed upper bounds for rate 1/2, K = seven, optimum code with QPSK on fully interleaved Rician channels with $\zeta = 0, 2, 5, 10, 20, \infty$.

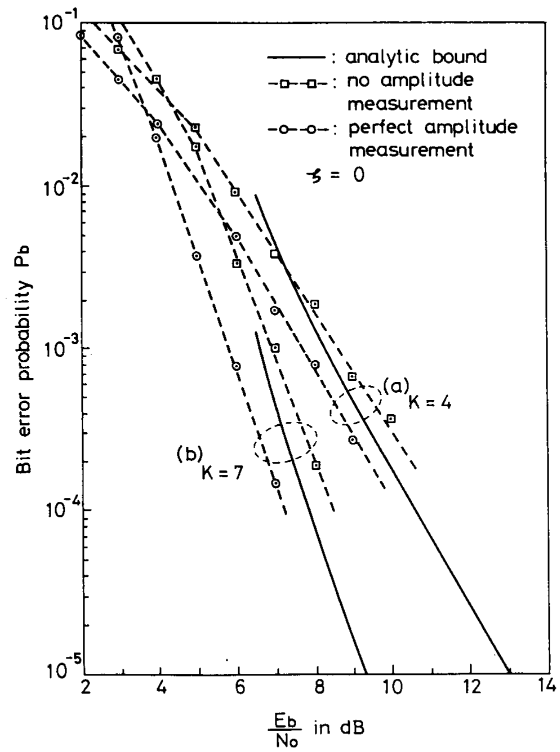

Fig. 7. Comparison of computer upper bounds and simulation results for selected rate 1/2 codes with QPSK on fully interleaved Rician channel with $\zeta = 0$.

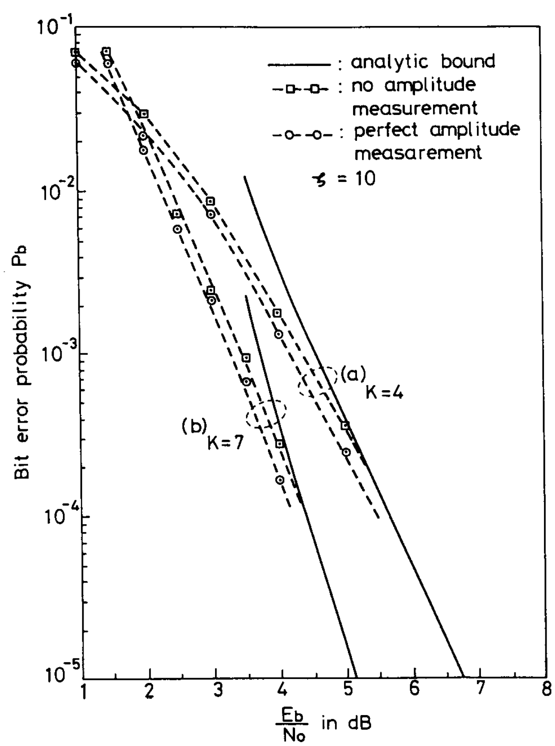

Fig. 8. Comparison of computer upper bounds and simulation results for selected rate 1/2 codes with QPSK on fully interleaved Rician channel with $\zeta = 10$.

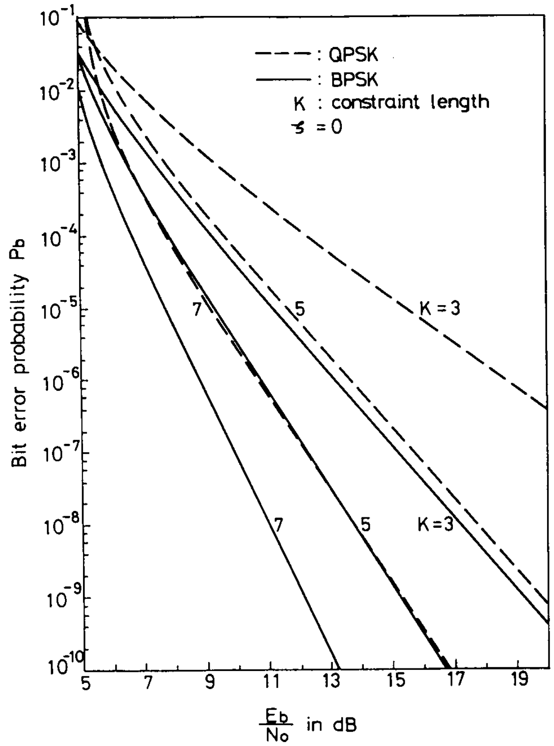

Fig. 9. Performance comparison (using upper bounds) between the selected rate 1/2 codes with QPSK and that with BPSK on fully interleaved Rician channel with $\zeta = 0$.

[3] is corrected here as

$$P_b \le P_d Z^{-d} \left. \frac{\partial T(D, I)}{\partial I} \right|_{I=1, D=z} \tag{17}$$

where

$$P_d = E\left[Q\left(\sqrt{\frac{E_b}{N_0} \sum_{i=1}^{d} a_i^2} \right) \right] \tag{18}$$

$$Z = \frac{1}{1 + \frac{E_b}{2N_0}\frac{1}{1+\zeta}} \exp\left(\frac{-\frac{E_b}{2N_0}\frac{\zeta}{1+\zeta}}{1 + \frac{E_b}{2N_0}\frac{1}{1+\zeta}} \right). \tag{19}$$

Here d denotes the minimum free distance of the code employed. This analytic bound is also asymptotically tight. Performance comparison between the selected codes with QPSK modulation and that with BPSK are shown in Figs. 9 and 10 for channels with $\zeta = 0$ and 10, respectively. Simulation results for K = four and seven codes with QPSK and that with BPSK are also provided in Fig. 11 and 12, respectively, for channel with $\zeta = 10$. It is found that, for severe fading, the performance of rate 1/2 convolutional codes with QPSK is worse than that with BPSK. However, for medium fading, relative performance degradation is slight. Moreover, when code constraint length is increased, the relative degradation is improved.

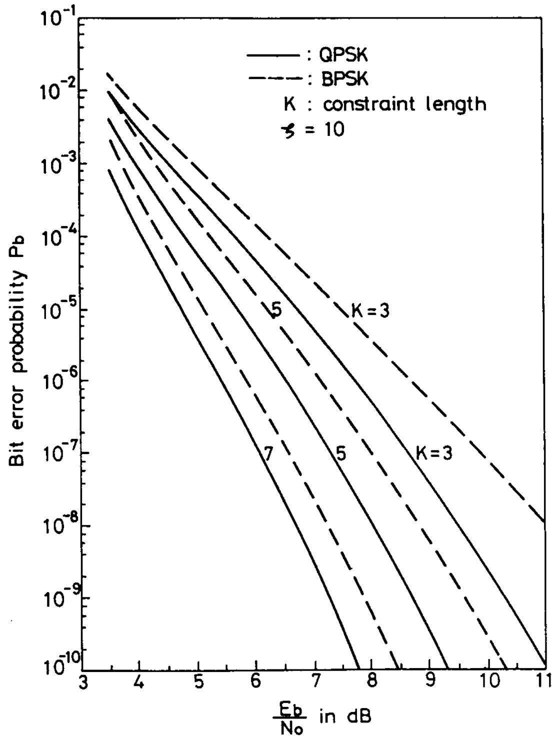

Fig. 10. Performance comparison (using upper bounds) between the selected rate 1/2 codes with QPSK and that with BPSK on fully interleaved Rician channel with $\zeta = 10$.

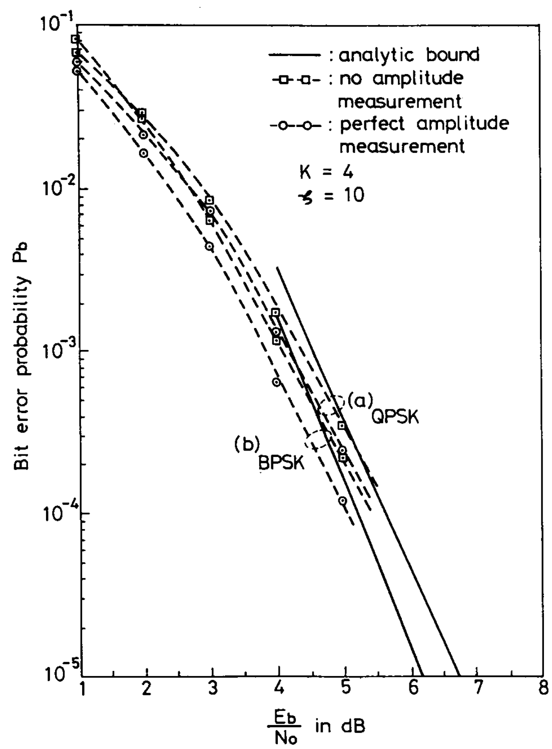

Fig. 11. Performance comparison (using simulation results) between K = four, rate 1/2, code with QPSK and that with BPSK on fully interleaved Rician channel with $\zeta = 10$.

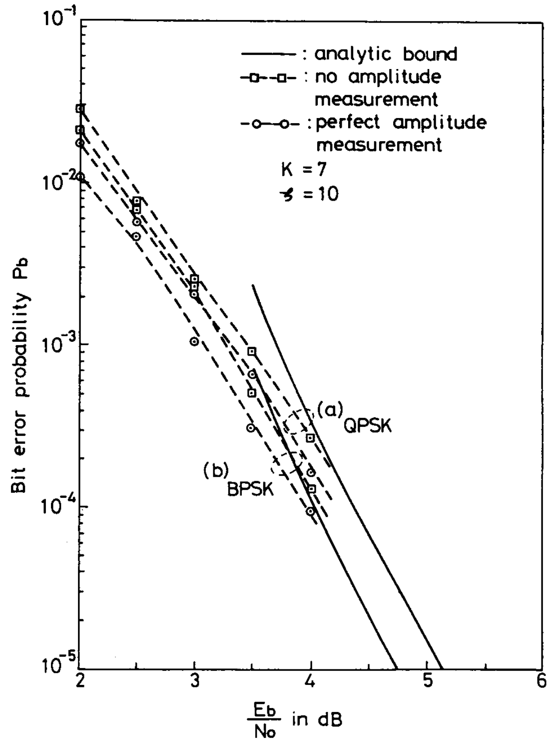

Fig. 12. Performance comparison (using simulation results) between K = seven, rate 1/2, code with QPSK and that with BPSK on fully interleaved Rician channel with $\zeta = 10$.

VI. Conclusion

In this paper, the bit error probability performance of rate 1/2 short constraint length optimum codes in conjunction with QPSK modulation and maximum likelihood Viterbi decoding on fully interleaved Rician fading channels has been studied. By applying the generating function union bounding approach, we have developed an analytic upper bound on the bit error probability performance under the assumption of using Viterbi decoding which makes perfect channel amplitude measurement. Bit error probability performance of selected short constraint length codes was evaluated numerically using the developed bound. We also provided computer simulation results for examining the tightness of the developed bound and for observing the influence of perfect amplitude measurement on the performance of Viterbi decoder. Results indicate that the derived bound is asymptotically tight and the performance of Viterbi decoder without amplitude measurement is comparable to that with perfect measurement in most cases, except in the severe fading channels. In comparison with the same codes with BPSK modulation, rate 1/2 convolutional codes with QPSK modulation and Viterbi decoding can provide effective error-control protection without sacrificing bandwidth efficiency and the relative performance degradation is slight when channel fading is not severe and code constraint length is sufficiently long.

Appendix I

For ML Viterbi decoder with perfect amplitude measurement, the likelihood function is denoted by $\Pr(\boldsymbol{y} \mid \boldsymbol{x}, \boldsymbol{a})$, where

$\boldsymbol{y}$ is the received sequence of decision variables, $\boldsymbol{x}$ is the transmitted sequence, and $\boldsymbol{a}$ is the measured fading amplitude sequence. The ML decoder compares all the likelihood functions and decides in favor of the maximum. Hence the decision rule between transmitted sequences $\boldsymbol{x} = \{x_i\}$ and $\boldsymbol{x}' = \{x_i'\}$ given the received sequences $\boldsymbol{y} = \{y_i\}$ and $\boldsymbol{a} = \{a_i\}$ is

$$\hat{\boldsymbol{x}} = \boldsymbol{x}', \qquad \text{if } \Pr(\boldsymbol{y}|\boldsymbol{a}, \boldsymbol{x}) < \Pr(\boldsymbol{y}|\boldsymbol{a}, \boldsymbol{x}') \tag{20}$$

where $\hat{\boldsymbol{x}}$ denotes the estimated sequence of the decoder. Because of statistical independence, this is equivalent to

$$\hat{\boldsymbol{x}} = \boldsymbol{x}', \qquad \text{If} \sum_i \ln p(y_i|a_i, x_i) < \sum_i \ln p(y_i|a_i, x_i'). \tag{21}$$

With y_i specified by (8), the conditional probability density function $p(y_i|a_i, x_i)$ is given by

$$p(y_i|a_i, x_i) = \frac{1}{\sqrt{2\pi}} \exp\left\{ -\frac{\left(y_i - \sqrt{\frac{E_b}{N_0}} a_i x_i\right)^2}{2} \right\}. \tag{22}$$

For rate 1/2 convolutional codes with Gray mapping into QPSK, we have $|x_i| = |x_i'|$. Further simplification of (21) leads to the desired result

$$\hat{\boldsymbol{x}} = \boldsymbol{x}', \qquad \text{if} \sum_i a_i y_i (x_i - x_i')^* + a_i y_i^* (x_i - x_i') < 0 \tag{23}$$

where the asterisk denotes the operation of complex conjugate. This is the form of decision rule that will be used in Appendix II to derive the pairwise error probability. Another equivalent form is given below:

$$\begin{aligned} \hat{\boldsymbol{x}} = \boldsymbol{x}' \qquad & \text{if} \sum_i a_i [\operatorname{Re}(y_i) \operatorname{Re}(x_i) \\ & + \operatorname{Im}(y_i) \operatorname{Im}(x_i)] < \sum_i a_i [\operatorname{Re}(y_i) \operatorname{Re}(x_i') \\ & + \operatorname{Im}(y_i) \operatorname{Im}(x_i')] \end{aligned} \tag{24}$$

where Re(#) and Im(#) represent the real and imaginary parts of the variable #, respectively. With $a_i = 1$, (24) becomes the one usually employed in the conventional ML Viterbi decoder (decoder without amplitude measurement).

Appendix II

If the estimated sequence $\hat{\boldsymbol{x}}$ differs from the transmitted sequence $\boldsymbol{x} = \{x_i\}$, with $x_i = 1$, (corresponding to the all-zero message) in exact k symbol positions and there are k_1 symbols with value $\pm j$ and k_2 symbols with value -1, then by (23) we have

$$\sum_{i=1}^{k} a_i y_i (1 - \hat{x}_i)^* + a_i y_i^* (1 - \hat{x}_i) \triangleq 2\left(\sum_{l=1}^{k_1} M_l + \sum_{m=1}^{k_2} M_m\right) < 0 \tag{25}$$

where

$$M_l = \sqrt{\frac{E_b}{N_0}} a_l^2 + a_l N_{cl} < a_l N_{sl} \tag{26a}$$

$$M_m = 2\left(\sqrt{\frac{E_b}{N_0}} a_m^2 + a_m N_{cm}\right). \tag{26b}$$

Here N_{ci} and N_{si} are the quadrature components of Gaussian noise N_i. Hence random variable $U = \sum_{l=1}^{k_1} M_l + \sum_{m=1}^{k_2} M_m$ is also Gaussian distributed with mean η_u and variance σ_u^2 given by

$$\eta_u = \sqrt{\frac{E_b}{N_0}} \left(\sum_{l=1}^{k_1} a_l^2 + 2\sum_{m=1}^{k_2} a_m^2\right) \tag{27a}$$

$$\sigma_u^2 = \sum_{l=1}^{k_1} a_l^2 + 2\sum_{m=1}^{k_2} a_m^2. \tag{27b}$$

The conditional pairwise error probability for the incorrect sequence with error pattern (k_1, k_2) is just

$$\begin{aligned} P_{k_1 k_2|a} &= \Pr(U < 0) \\ &= Q(\eta_u/\sigma_u) \\ &= Q\left[\sqrt{\frac{E_b}{N_0}\left(\sum_{l=1}^{k_1} a_l^2 + 2\sum_{m=1}^{k_2} a_m^2\right)}\right]. \end{aligned} \tag{28}$$

The unconditional pairwise error probability can then be determined by averaging over the random variables of $\boldsymbol{a}$ with the result

$$P_{k_1 k_2} = E\left[Q\left(\sqrt{\frac{E_b}{N_0}\left(\sum_{l=1}^{k_1} a_l^2 + 2\sum_{m=1}^{k_2} a_m^2\right)}\right)\right]. \tag{29}$$

Because (29) is hard to evaluate, further manipulation is required. Making use of the inequality $Q(\sqrt{x}) \le 1/2 \exp(-x/2)$ for $x \ge 0$ in (29), we obtain

$$P_{k_1 k_2} \le E\left[\frac{1}{2}\exp\left(-\frac{E_b}{2N_0} q_l\right) \cdot \exp\left(-\frac{E_b}{N_0} q_m\right)\right] \tag{30}$$

where, by definition, $q_l = \sum_{l=1}^{k_1} a_l^2$ and $q_m = \sum_{m=1}^{k_2} a_m^2$. Since a_m is Rician distributed, q_m is a noncentral chi-square-distributed random variable with characteristic function

$$\psi(j\alpha) = E[\exp(j\alpha q_m)] = \frac{1}{(1 - j2\alpha\sigma^2)^{k_2}} \exp\left(\frac{j\alpha \sum_{i=1}^{k_2} \gamma^2}{1 - j2\alpha\sigma^2}\right). \tag{31}$$

Recalling the normalization constraint (6) and the definition of parameter $\zeta = \gamma^2/2\sigma^2$, (30) can be simplified as

$$P_{k_1k_2} \leq \frac{1}{2} Z_1^{k_1} Z_2^{k_2} \tag{32}$$

where

$$Z_1 = \frac{1}{1 + \frac{N_b}{2N_0}\frac{1}{1+\zeta}} \exp\left(\frac{-\frac{E_b}{2N_0}\frac{\zeta}{1+\zeta}}{1 + \frac{N_b}{2N_0}\frac{1}{1+\zeta}}\right) \tag{33a}$$

$$Z_2 = \frac{1}{1 + \frac{E_b}{N_0}\frac{1}{1+\zeta}} \exp\left(\frac{-\frac{E_b}{N_0}\frac{\zeta}{1+\zeta}}{1 + \frac{E_b}{N_0}\frac{1}{1+\zeta}}\right). \tag{33b}$$

When (32) is used for deriving the bit error probability performance bound, a loose bound will result. In order to obtain a tighter bound, all the error pattern associated with a convolutional code are further examined. A computer program has been developed for this purpose. For rate 1/2 codes with constraint length K = three to eight, the minimum values of k_1 and k_2 denoted by d_1 and d_2, respectively, have been found and listed in Table I.

Making use of the inequality $Q(\sqrt{x+y}) \leq Q(\sqrt{x}) \exp(-y/2)$ for $x, y \geq 0$ in (29), we obtain

$$\begin{aligned} P_{k_1k_2} &\leq E\left[Q\left(\sqrt{\frac{E_b}{N_0}\left(\sum_{l=1}^{d_1} a_l^2 + 2\sum_{m=1}^{d_2} a_m\right)}\right) \cdot \exp\left(-\frac{E_b}{2N_0}\left(\sum_{l=d_1+1}^{k_1} a_l^2 + 2\sum_{m=d_2+1}^{k_2} a_m^2\right)\right)\right] \\ &\leq \underbrace{E\left[Q\left(\sqrt{\frac{E_b}{N_0}\left(\sum_{l=1}^{d_1} a_l^2 + 2\sum_{m=1}^{d_2} a_m^2\right)}\right)\right]}_{C} Z_1^{k_1-d_1} Z_2^{k_2-d_2}. \end{aligned} \tag{34}$$

Applying (34) to derive the performance bound will result a tight bound. However, the evaluation of C is still a problem.

TABLE I
MINIMUM VALUES OF k_1 AND k_2 AND MINIMUM FREE DISTANCE OF RATE 1/2, K = THREE TO EIGHT CONVOLUTIONAL CODES

Constraint Length (K)	Minimum Value of k_1 (d_1)	Minimum Value of k_2 (d_2)	Minimum Free Distance (d)
3	1	2	5
4	2	2	6
5	2	2	7
6	2	2	8
7	2	2	10
8	3	2	10

Hence the result given below is used instead.

$$\begin{aligned} P_{k_1k_2} &\leq E\left[Q\left(\sqrt{\frac{2E_b}{N_0}\sum_{m=1}^{d_2} a_m^2}\right)\right] Z_1^{k_1} Z_2^{k_2-d_2} \\ &\leq \underbrace{E\left[Q\left(\sqrt{\frac{2E_b}{N_0}q}\right)\right]}_{C_0} Z_2^{-d_2} Z_1^{k_1} Z_2^{k_2}. \end{aligned} \tag{35}$$

Since $q = \sum_{m=1}^{d_2} a_m^2$ is a noncentral chi-square-distributed random variable with $2d_2$ degree of freedom, distribution function of q is given by

$$f(q) = \frac{1}{2\sigma^2}\left(\frac{q}{d_2\gamma^2}\right)^{\frac{d_2-1}{2}} \exp\left(-\frac{d_2\gamma^2 + q}{2\sigma^2}\right) \cdot I_{d_2-1}\left(\frac{\sqrt{d_2 q}\gamma}{\sigma^2}\right) \tag{36}$$

where $I_d(\cdot)$ is the modified Bessel function of the first kind of order d. We then have

$$E\left[Q\left(\sqrt{\frac{2E_b}{N_0 q}}\right)\right] = \int_0^\infty Q\left(\sqrt{\frac{2E_b}{N_0}q}\right) f(q)\,dq. \tag{37}$$

The integration in (37) can be computed numerically.

REFERENCES

[1] F. Davarian, "Fade margin calculation for channels impaired by Rician fading," *IEEE Trans. Veh. Technol.*, vol. VT-34, pp. 41–44, Feb. 1985.

[2] J. W. Modestino and S. Y. Mui, "Convolutional code performance on the Rician fading channel," *IEEE Trans. Commun.*, vol. COM-24, pp. 592–606, June 1976.

[3] J. G. Dunham and K.-H. Tzou, "Performance bounds for convolutional codes on Rician fading channels," in *Proc. Int. Conf. Commun.*, 1981, vol. 1, pp. 12.4.1–12.4.5.

[4] J. Hagenauer, "Viterbi decoding of convolutional codes for fading- and burst-channels," in *Proc. Int. Zurich Seminar Dig. Commun.*, Zurich, 1980, pp. G.2.1–G.2.7.

[5] R. Schweikert and J. Hagenauer, "Channel modeling and multipath compensation with forward error correction for small satellite ship earth station," in *Proc. Sixth Int. Conf. Dig. Satell. Commun.*, Phoenix, AZ, 1983, pp. XII-32–XII-38.

[6] Y.-L. Chen and C.-H. Wei, "Performance bounds of rate 1/2 convolutional codes with QPSK on Rayleigh fading channel," *Electron. Lett.*, vol. 22, pp. 915–917, Aug. 1986.

[7] —, "Performance evaluation of convolutional codes with MPSK on Rician fading channels," *Inst. Elec. Eng. Proc.*, pt. F., vol. 134, no. 2, pp. 166–173, Apr. 1987.
[8] A. Ghasis and P. Branch, "Future development of the INMARSAT system," in *Proc. 3rd Inst. Elec. Eng. Int. Conf. Satellite Syst. for Mobile Commun. and Navigation,* 1983, pp. 207–211.
[9] A. J. Viterbi, "Convolutional codes and their performance in communications," *IEEE Trans. Commun. Technol.*, vol. COM-19, pp. 751–771, Oct. 1971.
[10] K. J. Larsen, "Short convolutional codes with maximum free distance for rate 1/2, 1/3, and 1/4," *IEEE Trans. Inform. Theory,* vol. IT-19, pp. 371–372, May 1973.

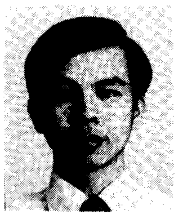

Yuh-Long Chen (S'85–M'86) was born in Taichung, Taiwan, Republic of China, on November 14, 1950. He received the B.S.E.E. degree from National Chiao Tung University, Hsin-Chu, Taiwan, in 1974, the M.S.E.E. degree from National Taiwan University, Taipei, Taiwan, in 1978, and the Ph.D. degree in electronics engineering from National Chiao Tung University in 1987.

From 1974 to 1976 he served in Chinese Navy. Since July 1978 he has been with Chung Shan Institute of Science and Technology, Lung-Tan, Taiwan. His research interests include digital modulation techniques and channel coding applications, in particular for mobile communication channels.

Che-Ho Wei (S'73–M'76–M'79–SM'87) was born in Taiwan, Republic of China, in 1946. He received the B.S.E.E. and M.S.E.E. degrees from National Chiao Tung University, Hsin-Chu, Taiwan in 1968 and 1970, respectively, and the Ph.D. degree from the University of Washington, Seattle, in 1976.

From 1976 to 1979 he was an Associate Professor at National Chiao Tung University, where he is now a Professor of the Institute of Electronics. His research interest areas include active and digital filter design, digital signal processing, and adaptive filtering.